CAV2021
11th International Symposium on Cavitation
May 10-13, 2021, Daejon, Korea

Prediction of Developed Tip Vortex Cavitation via a Panel Method

Seungnam Kim[1]* and Spyros A. Kinnas[1]

[1]Ocean Engineering Group,
Dept. of Civil, Architectural and Environmental Engineering,
The University of Texas at Austin, TX, 78712, U.S.

Abstract: In this paper, a panel method is adopted to model the unsteady developed tip vortex cavitation in the case of hydrofoil and propeller problems. A finite tip vortex core is placed at the tip of trailing wake, which is fully aligned to the local flow by satisfying the force free condition. The boundary value problem is solved on the hydrofoil (or propeller blade), together with the surfaces beneath the cavitation for velocity potentials and cavity sources respectively. The developed tip vortex cavitation is initially assumed as a cylindrical solid wall with a constant radius, then an elaborate iterative scheme adjusts the overall shape in both the streamwise and radial directions, by satisfying appropriate boundary conditions. During the process, local pressures are enforced to match the vapor pressure on the cavitating surfaces. The method is first applied to a 3D hydrofoil subject to the uniform inflow with a non-zero angle of attack and then to a partially cavitating propeller subject to the non-axisymmetric effective inflow. Comparisons are made qualitatively on the predicted cavity patterns with observations in the cavitation tunnel, and quantitatively on the predicted pressures to verify the feasibility and accuracy of the proposed method.

Keywords: Developed tip vortex cavitation; Sheet cavitation; Boundary element method; Unsteady wake alignment scheme

1. Introduction

Flow around blade tip, from the pressure side to suction side, produces tip vortex that flows from the blade tip to downstream. The tip vortex cavitation usually appears downstream in a detached form, and as the loading imposed near the tip increases, the detached cavitation approaches closer to the blade and eventually becomes fully developed tip vortex cavitation. The developed tip vortex cavitation in most occasions arises together with the sheet cavitation on the blade, and both are known to be associated with high frequency noise generation [1]. Prediction of the cavitation thus has been crucial aspects not only for the assessment of propeller performance but for an effective control over the propeller-induced acoustics propagating all around the ambient medium.

In the past, the mainstream of propeller design was to avoid cavity inceptions for a range of operating conditions because the cavitation is far destructive to the propulsion system due to its intrinsic growth and collapse mechanism. Excessive pressures during the collapse stage, for example, cause pitting on the blade, which in turn accelerates surface erosion of the blade, ship hull, and appendages. Despite all these negativities, recent demand for high speed vessels has altered the past design philosophy to practically tolerating cavity volume to some degree, but instead opting for a high-speed cavitating propeller that could operate under high loading conditions. Such trend renders the accurate prediction of cavity inception and understanding its growth/collapse mechanism more essential in the assessment of propeller performance. In particular, effects of cavitation on the hull vibration and underwater noise have already grown up as major concerns in the propeller design, especially for life functions of marine mammals.

The work in this paper is a continuation of the article [2] and briefly encompasses recent modifications thereafter. For the sake of succinctness, a summary of a boundary element method (or, BEM) that provides

* Corresponding Author: Seungnam Kim (naoestar@utexas.edu)

foundation behind the present method will be skipped in this paper, leaving details of the BEM, wake alignment scheme, and governing equations of the present method in [2-4].

2. Methodology

2.1. Dynamic and kinematic boundary conditions

The method starts with the initial guess on the tip vortex geometry, which is given as a thin cylinder following streamlines of the fully aligned wake. The Bernoulli equation can be established with respect to the propeller fixed system to satisfy the dynamic boundary condition of a constant vapor pressure on the surfaces beneath the cavitation. By connecting the two points, i.e., one on the cavitating surface and the other on the shaft axis far upstream, we have

$$\frac{P_0}{\rho}+\frac{1}{2}(|U_W|^2+\omega^2 r^2)=\frac{\partial\phi}{\partial t}+\frac{P_v}{\rho}+\frac{1}{2}|\vec{q}_t|^2+gy_S, \tag{5}$$

where ρ is the fluid density; r the distance from the axis of rotation and $\vec{q}_t$ is the total cavity velocity. P_0 is the reference pressure far upstream; g the gravitational constant; y_S the vertical distance from the horizontal plane through the axis of rotation; U_W the inflow velocity and ω is the propeller angular velocity. By introducing the cavitation number $\sigma_n=\frac{P_0-P_v}{\frac{\rho}{2}n^2D^2}$ with n and D being the revolution per unit second and the propeller diameter respectively, Equation 5 can be rearranged for the total cavity velocity $\vec{q}_t$ on the surface of tip vortex cavity as follows:

$$|\vec{q}_t|^2=n^2D^2\sigma_n+|U_W|^2+\omega^2r^2-2gy_S-2\frac{\partial\phi}{\partial t}. \tag{7}$$

Combining Equation 7 with another equation for $\vec{q}_t$ in terms of directional derivatives of the perturbation potential ϕ and the inflow components along the curvilinear coordinates produces a quadratic equation, which will then be solved for the perturbation velocity $\frac{\partial\phi}{\partial v}$ on the cavity surface. Kinematic boundary condition will be applied on the tip vortex cavitation after solving the boundary value problem to adjust the cavity radii by requiring the total derivatives of the cavity surface vanish on the cavity surface.

2.2. Potential jump boundary conditions

The potential difference between the first ($m=1$) and the last ($m=M$; if M panels are assumed circumferentially) panels has to be equivalent to the potential jump across the wake surface. This is because the tip vortex cavitation is attached to the wake tip. However, the potential difference is not always equal to the potential jump (or, wake strength) as the velocity potentials are evaluated from $\frac{\partial\phi}{\partial v}$, which is not fully converged in earlier time steps. To resolve this, relative distance between the control points around the tip vortex cavity has to be adjusted iteratively. The kinematic boundary condition is first applied on the cavity shape at the current time step to update the cavity radii in both the streamwise and circumferential directions. Then, the overall cavity volumes are further adjusted through the potential jump condition based on the local vortex strengths. After the cavity radii are updated, $\frac{\partial\phi}{\partial v}$ on the control points are reevaluated due to the changes in the panel coordinates. This process is conducted iteratively at each time step until the cavity shape converges.

2.3. Treatment of the collapsed tip vortex cavitation

* Corresponding Author: Seungnam Kim (naoestar@utexas.edu)

Figure 1 shows an example of thickness variation along the cavity strand after the shape adjustment. A weak wake strength Γ shortens the cavity height in satisfying the boundary conditions, which brings the panels below the critical radius that could lead to a singularity behavior. The sections with such small radii are considered *no tip vortex cavity zone* where the tip vortex cavity is assumed collapsing. In the event the developed tip vortex cavity collapses, viscous core reappears and that cannot be captured by the present inviscid method. To handle this, the present method uses a semi-empirical criterion of the non-dimensional circulation $G_{R,min}$, which serves as the minimum vortex strength, below which the tip vortex cavity is considered collapsed and thus neglected in the BEM matrices.

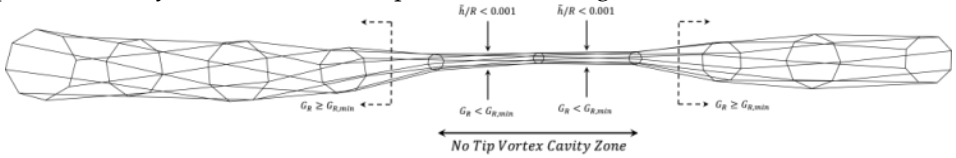

Figure 1. An example of tip vortex cavity with *no tip vortex cavity zone*. The criterion to determine the sections of *no tip vortex cavity zone* is when the local vortex core strength G_R is less than $G_{R,min}$.

3. Results

3.1. *Application to a rectangular hydrofoil*

The method is first applied to a 3D rectangular hydrofoil subject to the uniform inflow $\vec{U}_{in}$ with an angle of attack $\alpha^\circ = 5^\circ$ (Figure 2). As the foil geometry is symmetric about mid span, only the half span is presented in the figure. Aspect ratio is taken 8.0 and maximum thickness chord ratio t_{max}/C is given 0.01 with NACA0012 and $a = 0.8$ for foil cross section and mean camber line, respectively. In this case, 10 panels are assumed circumferentially in modeling the tip vortex cavitation. Figure 2 also shows cross sections of the initial/converged cavity shapes with pressure coefficients $\left(-C_p = \frac{P_0 - P_v}{\frac{\rho}{2} n^2 D^2}\right)$, plotted along its trajectory ($l/l_{max} = 0 \sim 1.0$). The predicted pressures are close to the cavitation number as intended except for the region near the foil tip. This is currently because the algorithm is not applicable to the conical bulb at the foil tip to avoid numerical issues.

3.2. Application to a partially cavitating propeller; DTMB N4148

In this section, the method is applied to a partially cavitating propeller DTMB N4148. Qualitative comparisons are made on the cavitation patterns between the experiment [5] and present method in Figure 3. The non-axisymmetric effective wake, taken from [6] is also shown, shifted a bit upstream for clarity.

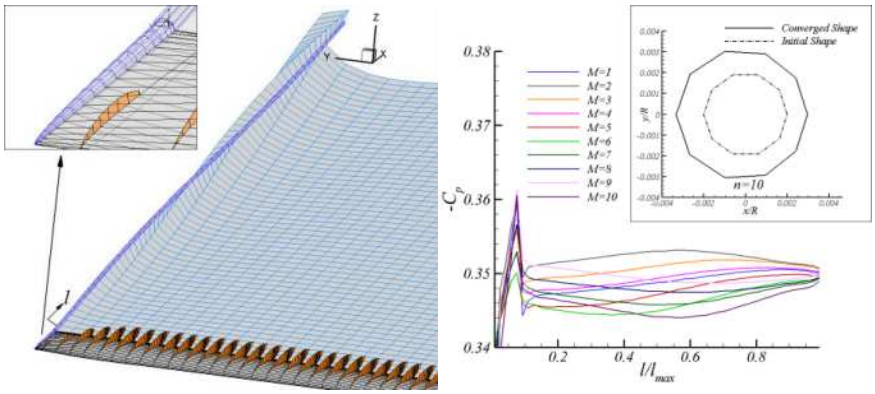

* Corresponding Author: Seungnam Kim (naoestar@utexas.edu)

Figure 2. Left, 3D rectangular hydrofoil with predicted sheet/tip vortex cavitation, along with the trailing wake at $\alpha = 5°$; Right, predicted surface pressures along the trajectory of the tip vortex cavitation: $\sigma_n = 0.35$.

As expected from the effective wake, cavity volumes increase as the key blade enters and passes the positive y region (note the propeller center is placed at $y = 0$) where the axial component of the incoming flow is relatively slower. In particular, the tip vortex cavitation detaches from the key blade beyond $\theta = 60°$ angular position as the vortex strength G_R falls below the minimum threshold thereafter. The tip cavity starts to reappear as the key blade turns around and re-enters the positive y region from $\theta = 300°$, and develops until the blade completely exits the wake peak region. In the same figure, the predicted cavity patterns are compared to the photographs taken in the cavitation tunnel [5]. Observations are made at $\theta = -30°$, $6°$, and $30°$ key blade positions, and the qualitative comparisons show they are in reasonable agreement with each other.

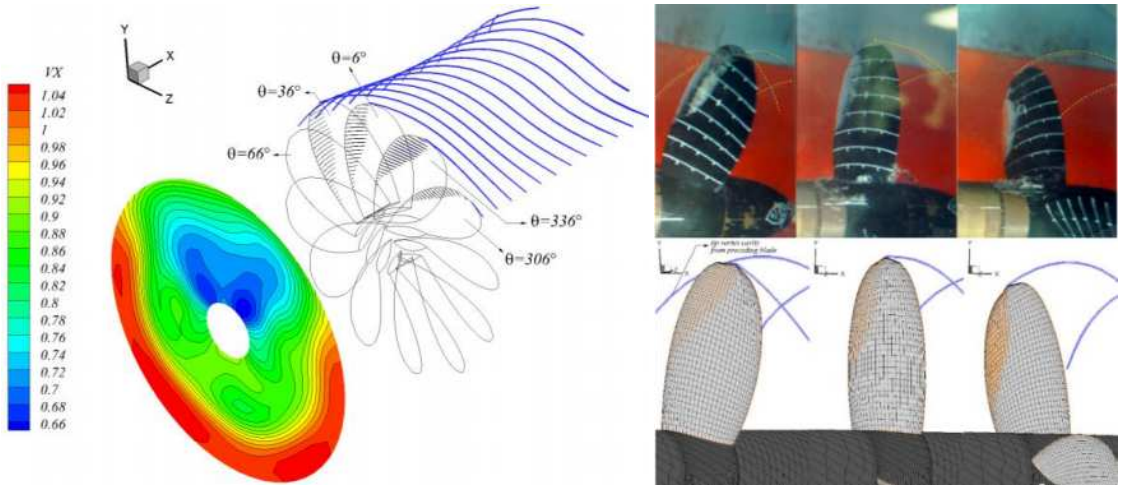

Figure 3. Left, geometry of DTMB N4148 propeller subject to the non-axisymmetric effective inflow and the predicted sheet/tip vortex cavitation, plotted at every 30°: $\sigma_n = 2.576$ and $J_s = 0.954$; Right, comparisons of the predicted cavitation by the present method with the observations (traced with yellow dashed lines): $\sigma_n = 2.576$, $J_s = 0.9087$ and $F_n = 9.159$.

Acknowledgments: Support for this research was provided by the U.S. Office of Naval Research (Grant Number N00014-18-1-2276; Dr. Ki-Han Kim) and by Phase VIII of the "Consortium on Cavitation Performance of High Speed Propulsors".

References

1. Calton, J. S., Marine Propellers and Propulsion; Butterworth-Heinemann: Oxford, 1994.
2. Kim, S.; Kinnas, S.A. Prediction of Unsteady Developed Tip Vortex Cavitation and Its Effect on the Induced Hull Pressures. *Journal of Marine Science and Engineering* **2020**, *8 (114)*, pp. 1-44.
3. Kim, S.; Kinnas, S.A.; Du, W. Panel Method for Ducted Propellers with Sharp Trailing Edge Duct with Fully Aligned Wake on Blade and Duct. *Journal of Marine Science and Engineering* **2018**, *6 (89)*, pp. 1-22.
4. Lee, H.; Kinnas, S.A. Application of BEM in the Prediction of Unsteady Blade Sheet and Developed Tip Vortex Cavitation on Marine Propellers. *Journal of Ship Research* **2004**, 48 (1), pp. 15-30.
5. Mishima, S.; Kinnas, S.A.; Egnor, D. The Cavitating Propeller Experiment (CAPREX), Phase I & II; Technical Report; Dept. of Ocean Engineering, MIT: Cambridge, MA, 1995.
6. Choi, J.; Kinnas, S.A. Prediction of Non-axisymmetric Effective Wake by a 3-D Euler Solver. *Journal of Ship Research* **2001**, 45 (1), pp. 13-33.

* Corresponding Author: Seungnam Kim (naoestar@utexas.edu)